DESIGN AND OPERATION OF A MICROMACHINED BUBBLE-JET CELL SORTER

Chung-Chu Chen[1], Jen-Shiang Wang[2], Stefan Zappe[2], Xiaojing Zhang[3], Olav Solgaard[2]
[1]Smart Sensor and Integrated Microsystems Program, Wayne State University, USA, [2]Department of Electrical Engineering, Stanford University, USA, [3]MIT Media Laboratory, Massachusetts Institute of Technology, USA
E-mail: chungchu@ieee.org

ABSTRACT

We present a high-speed microfluidic cell sorter employing embedded heaters and nozzles to generate deflecting jets to change the movement of the cells. We simulated the transient flow fields to validate the concept and optimize the sorter design. The simulation demonstrates a spatial switching windows corresponding to 1.1 times the switching chamber length. Experimental verification was obtained using micromachined devices characterized by stroboscopic measurements. With a 4.9 μs working period for the 20×20 μm^2 heaters that generate the deflecting jets, the sorter can potentially attain a working frequency of 50 kHz or higher. We built a scattered-light based optical system to detect moving particles and successfully performed sorting of 20 μm microspheres. This type of sorter is promising for micromanipulation of a variety of biological cells and inorganic particles.

Keywords: Bubble jet, Cell sorting, Microfluidics

INTRODUCTION

Flow cytometric cell sorting rapidly separates cells one at a time based on optical or other properties [1]. The most widely used method is droplet sorting. Drops containing desired cells are charged and separated with very high speed (tens of thousand cells per second) by electrostatic deflection [2]. The enclosed-type cell sorter has the advantages of lower cost and greater ease of use. Large cells and embryos can be sorted by mechanical switches, but this method suffers from slow sorting rates (hundreds cells per second or less) and large size [3]. Micromachined fluidic channels can replace conventional large flow chambers, and several research groups have reported using electro-osmosis [4], magnetic fields [5] and fluidic-switching [6] to manipulate cells. None of these previous reported micro sorting devices can provide a sorting speed comparable to that of the droplet sorter. In this paper we describe the design, simulation, fabrication and experimental verification of a micromachined thermal bubble-jet sorter capable of high speed cell sorting. Similar bubble actuators have been used to release particles from single-cell capture wells [7].

DESIGN

The schematic drawing of the bubble-jet sorter is shown in Fig. 1. The sorter is comprised of one cell inlet channel and two buffer inlet channels that all open into a switch chamber with two outlet channels. The buffer inlets are connected to a common buffer source. Each buffer channels is terminated in a firing chamber and a nozzle connected to the switch chamber. A micro heater is integrated on the wall of the firing chamber. Applying an electric pulse, one of the micro heaters can generate a micro thermal bubble. The volume expansion of the bubble will force the buffer liquid to pass through the nozzle and form a deflecting jet that pushes the selected cell toward the farther outlet.

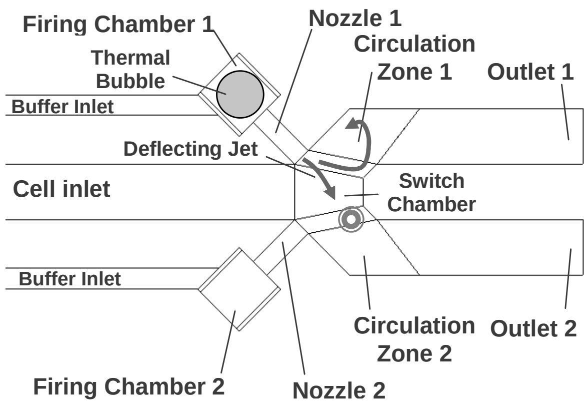

Fig. 1. Design of the high speed bubble-jet cell sorter.

Compared to other sorting mechanisms, this method has the following advantages:

1. No external electrostatic or magnetic fields are required.
2. No slow pressure valve or switch is required.
3. No moving parts will cause clogging or mechanical failure.

SIMULATIONS

We simulated the flow dynamics with the CFD-ACE$^+$ software to validate the sorter concept and optimize the channel geometries and flow parameters of the microfluidic sorter design. The study employed the volume-of-fluid (VOF) method for free-surface flows with surface tension to model the floating cell motion in the transient incompressible fluid flow. The moving-wall and grid-deformation methods simulate the motion of the thermal bubble actuator and the volume change of

TRANSDUCERS'05
The 13th International Conference on Solid-State Sensors, Actuators and Microsystems, Seoul, Korea, June 5-9, 2005
0-7803-8952-2/05/$20.00 ©2005 IEEE.

the firing chamber. The displacement of the actuator surface can be specified by an oscillating mathematical expression. The fluid-flow model solves the coupled time dependent continuity equation, the pressure-based Navier-Stokes equations, and the energy balance equation.

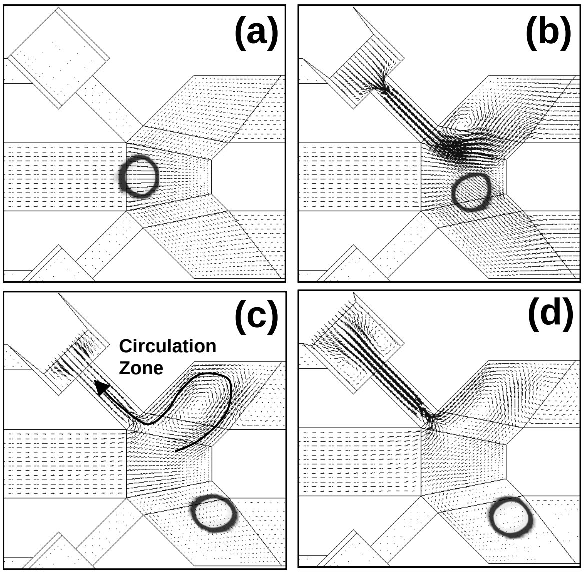

Fig. 2. Four consecutive instances of simulated cell sorting using deflecting jet.

Figure 2 shows four instances of transient results of the simulated cell sorting. The upper actuator was activated while the cell entered the switch chamber. The actuator displaced and expelled the liquid into the nozzle and formed jet which pushes the cell, as shown in Figs. 2(a-b). The actuator retracted after the cell left the switch chamber. A suction flow was formed to refill the firing chamber. Most of the refilling fluid came from the designated circulation zone as shown in Fig. 2-(c). The cell was prevented from being pulled back by the suction flow.

We performed a series of simulations to study the switching window of the jet sorter. The actuator was activated when the cell passed different locations. If the actuator was activated too early, the cell entered the switching chamber while the actuator already retreated. The suction effect around the nozzle pulled the cell toward the wrong direction. Figure 3(a) shows an example of failed switching with two overlapping instances (the earlier one in lighter tone). On the other hand, if the jet was activated too late, the cell had already reached the dividing wall. The jet then pushed the cell against the wall, which resulted in marginal sorting. As shown in Fig. 3(b), the cell was deformed (lighter) and split into two parts (darker). The larger part still moved in the right direction. Within the switching window, W_{SW}, the cell can be successfully switched to the correct outlet, as illustrated in Fig. 3(c). The switching window corresponds to 1.1 times the switching chamber length, L_C.

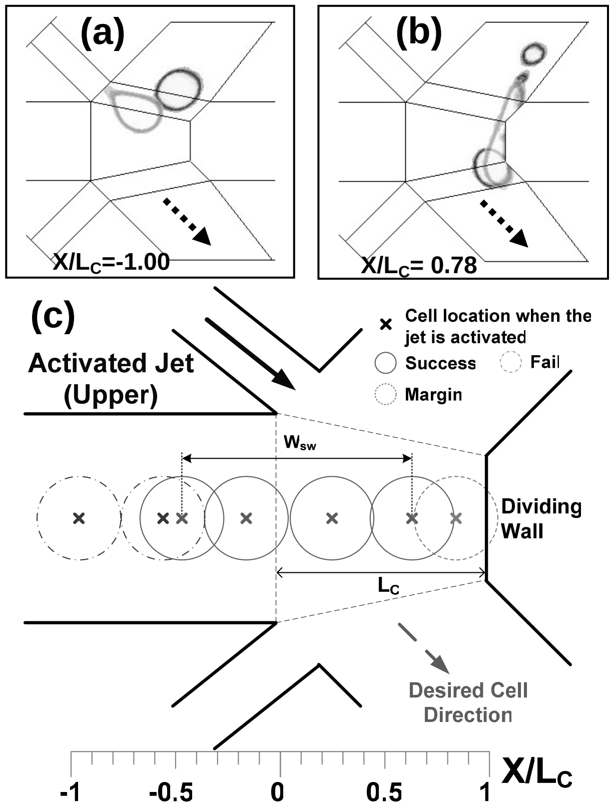

Fig. 3. (a)Failed sorting due to early activation of jet, (b) Marginal sorting due to late activation of jet, and (c) Switching window for the bubble-jet sorter.

FABRICATION

Figure 4 shows the major steps of the fabrication process. The front side of silicon wafer was patterned using standard photolithography and deep reactive ion etching (DRIE) to form the microfluidic channels. Another DRIE was performed on the back side to etch through the silicon wafer, as shown in Fig. 4(a). The etched openings provide connections to the microfluidic channels and access to the circuit pads. Pyrex wafers were used as the cover of the microfluidic channels to provide optical access of the laser light source and the photo detector. The bubble actuator circuits were also patterned on the Pyrex, as depicted in Fig. 4(b). The HF was used to etch 1-micron-deep trenches on the Pyrex wafers. A layer of 400Å titanium (Ti) was sputtered on the Pyrex and patterned by a lift-off process to construct the micro heaters. The conducting wires were made by successive sputtering and lift-off of 3000Å gold (Au). An insulating layer of 3000 Å silicon nitride was deposited on Pyrex by PECVD and then patterned by a plasma etch. Finally, the Pyrex wafers were anodically bonded to the Si wafers (Fig. 4(c)). All the heaters, conductors, and insulators were patterned in the Pyrex trenches in order to achieve better anodic bonding.

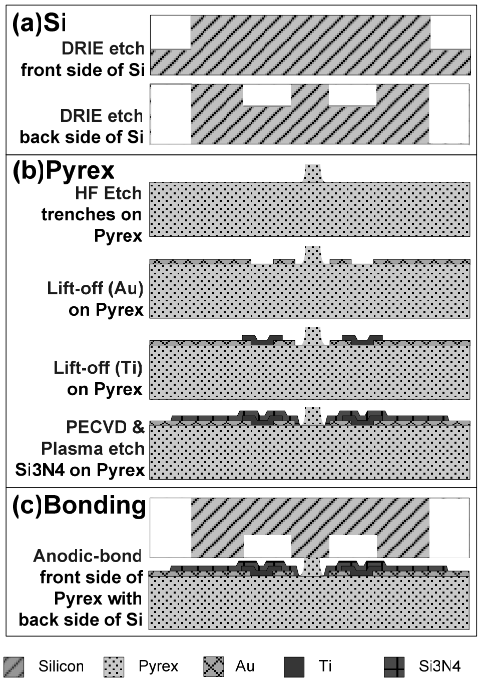

Fig. 4. Fabrication processes for (a) Si wafers, (b) Pyrex wafers, and (c) bonding.

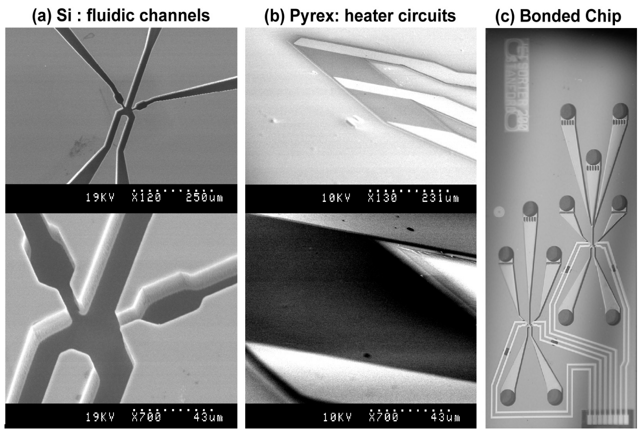

Fig. 5. SEM and photo of the fabricated device

SEMs of fabricated microfluidic channels and micro heaters are shown in the in Figs. 5(a) and 5(b). Figure 5(c) shows a sorter chip after dicing of the bonded Si and Pyrex wafers.

EXPERIMENTAL RESULTS

We built a stroboscopic system [8] to perform open-pool tests of the micro heaters and to characterize the bubble formation and power requirement. Three sizes of square micro heaters, 20 µm × 20 µm, 50 µm × 50 µm, and 100 µm × 100 µm, were tested for the heating conditions to produce bubbles with comparable size with each heater. Thermal bubbles generated by the microheaters are shown in Fig. 6(a)-(c). The bubble-generating conditions are listed in Table 1. The micro heaters need power densities on the order of 10^9 W/m^2 to form bubbles. The power density for the 100 µm square micro heater is slightly smaller, but a longer pulse width (15 µs) was needed. The total input energy and the duration of the bubble are both proportional to the heater size. With a 25% duty cycle for the 4.9 µs working period of the 20×20 µm^2 heater, the sorter can attain a 20 µs total period, i.e. a working frequency of 50 kHz. This sorting rate is comparable to the sorting speeds of much more complex and bulky stream-in-air droplet sorting systems (e.g. BD FACSAria™). Larger heaters may provide higher actuation force to push heavier particles, but lower operating frequency and sorting rate are expected.

Fig. 6. Visualized thermal bubbles for different sizes of micro heaters.

Table 1. Bubble generating conditions

Size (µm^2)	20×20	50×50	100×100
Resistance (Ω)	52.9	50.3	52.5
Current (A)	0.096	0.24	0.34
Pulse width (µs)	5	5	15
Power density (W/m^2)	1.22×10^9	1.16×10^9	6.07×10^8
Total energy (J)	2.44×10^{-6}	1.45×10^{-5}	9.10×10^{-5}
Bubble duration (µs)	4.9	9.5	27.3

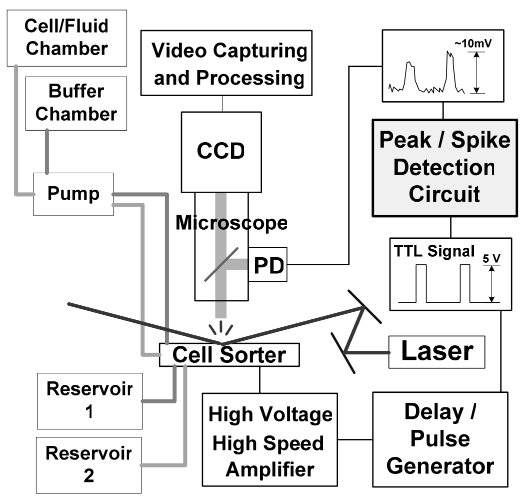

Fig. 7. Cell sorting experimental set-up.

The cell sorting experimental set-up shown in Fig. 7 was used to verify the function of the bubble-jet sorter.

An optical system was built to detect moving particles within the microfluidic channels and to generate the electrical signals for the micro heaters. The photo detector is set up to collect most of the scattered light from moving particles without picking up the reflected light from the channel walls. The acquired optical signals were reconditioned by a customized circuit for offset, amplification, peak detection, and generation of TTL triggering signals. The pulse/delay generator was fed with the TTL signals and was used to control the timing between detection and actuation. A high-speed and high-voltage amplifier adjusted the voltage of the delayed pulses to power levels suitable for the micro heaters.

With sorting speed reduced to enable video capture, continuous sorting of polystyrene microspheres to either one of the outlets at speed ranging from 1500 to 3500 μm/s was recorded. The eight successive video frames in Figs. 8(a-h) show a 20 μm microsphere entering the detection window and being pushed toward outlet 2 by the bubble jet on the opposite side. The microsphere was accelerated by the jet flow, as evidenced by the longer scattered-light trace near outlet 2 (lower right) in Figs. 8(g-h).

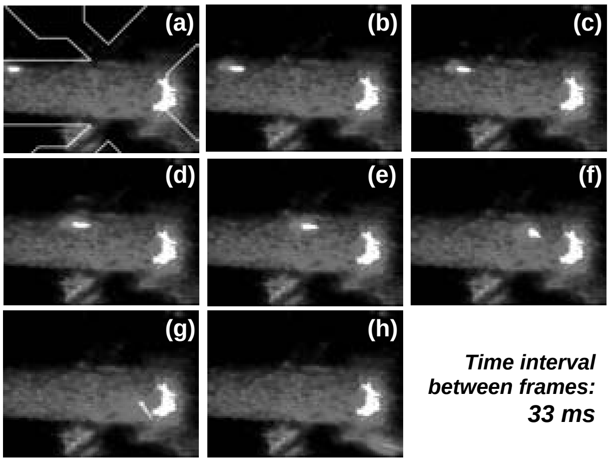

Fig. 8. Flow visualization of micro spheres sorting.

CONCLUSION

We have demonstrated the design, simulation, fabrication and operation of a high-speed microfluidic cell sorter. An embedded bubble-jet actuation technique was used to deflect the cell motion in the micro channels. CFD simulations demonstrated a switching window of 1.1 times the switching chamber length. Sorting devices were fabricated and stroboscopic measurements were taken to characterize the bubble actuators. Microheaters with a 20×20 μm^2 area and a 5 μs working period are promising for very high sorting rates. Successful sorting experiments were performed by detecting scattered laser light of the 20 μm microspheres. A natural extension of this work is to integrate on-chip photo detectors for more precise and higher-speed cell sorting.

ACKNOWLEDGEMENTS

Support for this research was provided by the Defense Advanced Research Projects Agency under contract MDA972-00-1-0032.

REFERENCES

[1] R.A. Hoffman and D.W. Houck, "Cell Separation Using Flow Cytometric Cell Sorting"; pp. 237-69, in Cells Separation Methods and Applications, Edited by D. Recktenwald and A.Radbruch, Marcel Dekker, Inc., New York, 1998.

[2] T. Lindmo, D.C. Peters, and R. Sweet, "Flow Sorters for Biological Cells"; pp. 162-70, in Flow Cytometry and Sorting, Edited by M. R. Melamed, T. Lindmo, and M. L. Mendelsohn, Wiley-Liss, New York, 1990.

[3] E.E.M. Furlong, D. Profitt, and M.P. Scott, "Automated Sorting of Live Transgenic Embryos," *Nat. Biotechnol.*, **19**, pp. 153-6 (2001).

[4] A.Y. Fu, C. Spence, A. Scherer, F.H. Arnold, S.R. Quake, "A Microfabricated Fluorescence-activated Cell Sorter," *Nat. Biotechnol.*, **17**, pp. 1109-11 (1999).

[5] C. Chaktranond, K. Fukagata, and N. Kasagi, "Mixing Enhancement in a Micro Serpentine Conduit for Cell Sorting," *5th Int. Conference on Multiphase Flow*, Yokohama, Japan, May 30 – Jun. 4, 2004.

[6] C.C. Chen, S. Zappe, O. Sahin, X.J. Zhang, M. Fish, M. Scott, and O. Solgaard, "Design and operation of a microfluidic sorter for Drosophila embryos," *Sensor Actuat. B-Chem.*, **102/1**, pp. 59-66 (2004).

[7] R.B. Maxwell, A.L. Gerhardt, M. Toner, M.L. Gray, and M.A. Schmidt, "A microbubble-powered bioparticle actuator," *J. Microelectromech. S.*, **12**, pp. 630-40 (2003).

[8] C.C. Chen, C.K. Chung, S.H. Chen, and T.M. Liou, 2004, "Flow Simulation and Visualization of a Micro Droplet Generator," *J. Flow Visual. Image Process.*, **11**, pp 54-65 (2004).